



LAWRENCE  
LIVERMORE  
NATIONAL  
LABORATORY

# M-ARIANE, an x-ray imaging system for implosion experiments on National Ignition Facility at ignition neutron yields

V. A. Smalyuk, J. Ayers, P. M. Bell, R. L. Benedetti, D. K. Bradley, C. Cerjan, J. Emig, G. Felker, S. M. Glenn, C. Hagmann, J. Holder, N. Izumi, J. D. Kilkenny, J. A. Koch, O. L. Landen, J. Moody, K. Piston, N. Simanovkaia

July 31, 2013

SPIE Optics & Photonics 2013  
San Diego, CA, United States  
August 25, 2013 through August 29, 2013

## **Disclaimer**

---

This document was prepared as an account of work sponsored by an agency of the United States government. Neither the United States government nor Lawrence Livermore National Security, LLC, nor any of their employees makes any warranty, expressed or implied, or assumes any legal liability or responsibility for the accuracy, completeness, or usefulness of any information, apparatus, product, or process disclosed, or represents that its use would not infringe privately owned rights. Reference herein to any specific commercial product, process, or service by trade name, trademark, manufacturer, or otherwise does not necessarily constitute or imply its endorsement, recommendation, or favoring by the United States government or Lawrence Livermore National Security, LLC. The views and opinions of authors expressed herein do not necessarily state or reflect those of the United States government or Lawrence Livermore National Security, LLC, and shall not be used for advertising or product endorsement purposes.

# M-ARIANE, an x-ray imaging system for implosion experiments on National Ignition Facility at ignition neutron yields

V.A. Smalyuk<sup>a</sup>, J. Ayers<sup>a</sup>, P. M. Bell<sup>a</sup>, R. L. Benedetti<sup>b</sup>, D. K. Bradley<sup>a</sup>, C. Cerjan<sup>a</sup>, J. Emig<sup>a</sup>, B. Felker<sup>a</sup>, S. M. Glenn<sup>a</sup>, C. Hagmann<sup>a</sup>, J. Holder<sup>a</sup>, N. Izumi<sup>a</sup>, J. D. Kilkenny<sup>b</sup>, J. A. Koch<sup>a</sup>, O. L. Landen<sup>a</sup>, J. Moody<sup>a</sup>, K. Piston<sup>a</sup>, N. Simanovskaia<sup>a</sup>

<sup>a</sup> Lawrence Livermore National Laboratory, 7000 East Ave, Livermore, USA 94550;

<sup>b</sup> General Atomics, San Diego, CA

## ABSTRACT

X-ray imaging diagnostics instruments will operate in a harsh ionizing radiation background environment during ignition experiments at the National Ignition Facility (NIF). These backgrounds consist of mostly neutrons and gamma rays produced by inelastic scattering of neutrons. An imaging system M-ARIANE, based on x-ray framing camera with film, has been designed to operate in such harsh neutron-induced background environments. Multilayer x-ray mirror and a shielding enclosure are the key components of this imaging system, designed to operate at ignition neutron yields of  $\sim 10^{18}$  on NIF. Modeling of the neutron- and gamma-induced backgrounds along with the signal and noise of the x-ray imaging system is presented.

**Keywords:** x-ray imaging, neutron-induced backgrounds

## 1. INTRODUCTION

Time-gated, x-ray imaging [1] is an essential diagnostic of spherical implosions in Inertial Confinement Fusion (ICF) experiments [2] currently underway on the National Ignition Facility (NIF) [3].

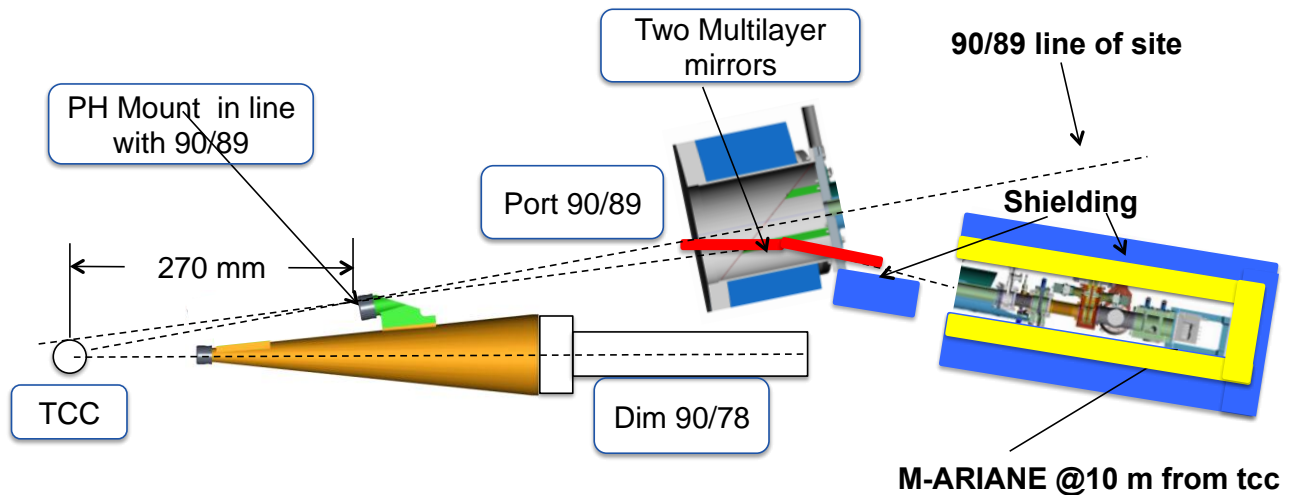


Figure 1: M-ARIANE consists of a 10-μm diameter pinhole array at 27 cm from the target chamber center, two multilayer x-ray mirrors, operating at 2-degree angle of incidence. They direct 9-keV x-ray images to a framing camera outside target chamber wall at 10 meters from the target chamber center. The framing camera is shielded by the combination of lead (yellow color) and boron-polyethylene (blue color) shielding.

It provides temporally resolved x-ray images used for measuring shape, size, and burn history of the compressed core of imploding cryogenic deuterium-tritium (DT) capsules [1,2]. The symmetry and the size of the fuel during implosion are two key parameters used for an optimization in the ICF experiments [2,3]. The most-used x-ray imagers in ICF consist of the pinhole array and a framing camera [4,5]. The pinhole array produces a large number of x-ray images on the micro-channel plate (MCP) of the framing camera. Temporal gating of the MCP allows the x-ray images to be recorded at different times. X-rays, incident on the MCP, are converted into electrons and then multiplied inside the MCP [4,5]. After leaving the MCP, the electrons are converted into visible photons in a phosphor plate. These photons are transported in a fiber-optic plate (FOP) to a detector, a CCD, or a film [4,5].

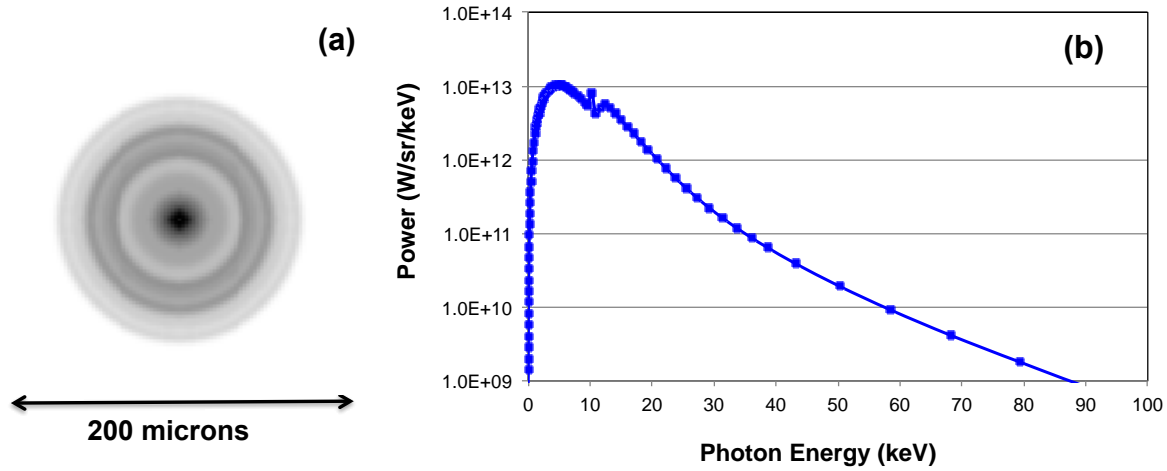


Figure 2: (a) Predicted core image at peak emission of cryogenic DT implosion with DT neutron yield of  $2 \times 10^{18}$ . (b) Spectral power of x-rays emitted by a core at peak emission.

There are three types of gated imagers available at NIF now. The gated x-ray detectors (GXD's) can operate at DT neutron yields up to  $Y_n \sim 10^{13}$  with CCD's at a standoff of 1.3 meters from the target chamber center (TCC) [1]. Hardened gated x-ray images (hGXI's) use film instead of CCD and can operate at DT neutron yields up to  $Y_n \sim 10^{15}$  with the same standoff. [6]. ARIANE (Active Readout In A Neutron Environment) is an x-ray imager with a framing camera located outside the target chamber walls, was designed [7,8] to operate at yields up to  $Y_n \sim 3 \times 10^{16}$ . Similar instruments have also been used at several other ICF facilities with moderate DT neutron yields up to  $Y_n \sim 10^{13}$  when neutron-induced noise on CCD and film and long-term damage to the CCD's were manageable. In the future, much higher neutron yields above  $Y_n \sim 10^{18}$  are expected at the NIF and LMJ facilities [3] requiring imagers with increased radiation hardness.

A schematic of one such a gated imager is shown in Fig.1. It is called M-ARIANE (where M stands for a mirror) which is designed to operate at DT ignition neutron yields up to  $Y_n \sim 10^{18}$  on NIF. It is a modification of the current imager ARIANE [7-9] with additional multilayer x-ray mirror and additional shielding against neutron and gamma ray backgrounds. M-ARIANE consists of a pinhole array positioned at 27 cm from TCC on a DIM snout. GXD and hGXI imagers have pinholes located at closer distance of 8 cm, so the x-ray collection efficiency of the ARIANE will be about 10 times lower, compared to images used for lower yields. The framing camera will be positioned outside target chamber wall at about 10 meters from TCC, providing an object magnification of about  $\sim 36$ .

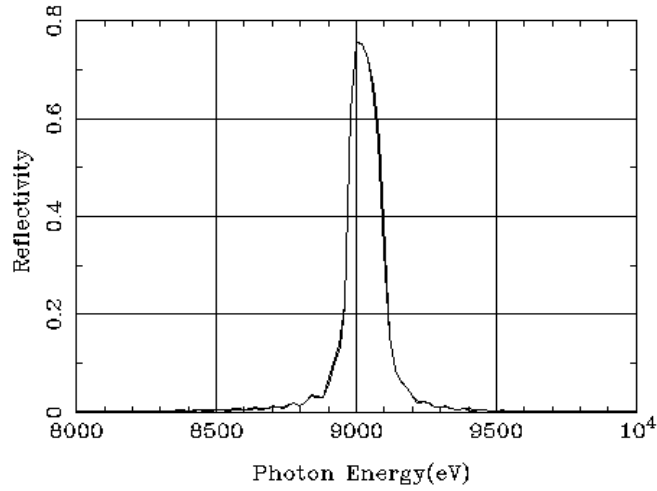


Figure 3: Reflectivity as a function of the photon energy for the W/C multilayer mirror with a period of 20Å, number of layers  $N=300$ , and an inter-diffusion thickness of 2Å.

Two x-ray mirrors (both 25 cm long and 5 cm wide) direct x-rays to the framing camera located behind the target chamber wall that provides shielding against neutrons and gamma rays. Addition shielding, shown in Fig. 1, provides necessary reduction in neutron and gamma ray backgrounds to operate at yield up to  $Y_n \sim 10^{18}$ . This article describes modeling of the effects of the neutron-induced backgrounds on image quality and shows the effect of the noise and resolution on the measured images. Section 2 describes the expected images, signal levels and photometrics of implosion x-ray emission. Section 3 describes sources of the neutron-induced backgrounds and their mitigation by the shielding. Section 4 shows the effects of these backgrounds on image quality at DT neutron yields up of  $Y_n \sim 2 \times 10^{18}$ . Section 5 summarizes the results.

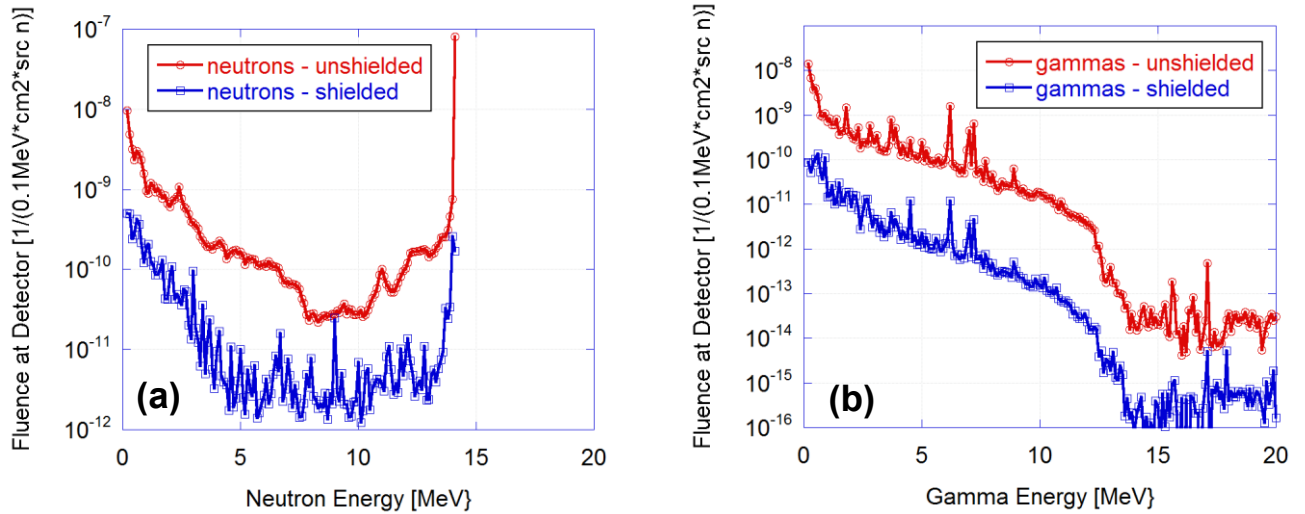


Figure 4: Calculated (a) neutron and (b) gamma fluence at the framing camera location in the ARIANE detector (red curves) and M-ARIANE detector (blue curves).

## 2. SIGNAL PREDICTIONS AND PHOTOMETRICS

Figure 2(a) shows the predicted image of the implosion core at the peak of x-ray emission. The image shows structure that is required to be measured for understanding of the implosion. The calculated spectral power as a function of x-ray photon energy of the core at peak emission is shown in Fig. 2(b). The predicted total yield in this implosion is 6 MJ, corresponding to the DT neutron yield of  $Y_n \sim 2 \times 10^{18}$ . Reduction in calculated spectral power at  $\sim 11$  keV is due to Ge K-edge absorption of the core emission in a colder Ge-doped CH shell surrounding a hot DT core. The reduction of the spectral power right below  $\sim 10$  keV is due to the absorption by both Ge and CH of the shell.

Figure 3 shows calculated reflectivity of the multilayer mirror as a function of the photon energy. The mirror is used to direct x-rays to the framing camera located behind the target chamber wall in the special shielding enclosure to protect it against neutron-induced backgrounds. W/C multilayer mirror has a period of 20 Å, number of layers  $N=300$ , and an inter-diffusion thickness of 2 Å. It is used at 2-degree angle of incidence to reflect  $\sim 9$  keV x-rays with  $\sim 150$  eV x-ray bandwidth, at peak reflectivity of  $\sim 0.7$ . The calculated spectral power at 9 keV is  $\sim 1 \times 10^{13}$  W/(sr\*keV), as shown in Fig. 2(b). The solid angle of 10- $\mu$ m pinhole placed at 27 cm from the object is  $\sim 1 \times 10^{-9}$  sr. The transmission of 2.5 mm Kapton filter is  $\sim 0.3$  at photon energy of 9 keV. Using the 100-ps integration time of the framing camera, the magnification of 36, and the detector square pixel size of  $20 \times 20 \mu\text{m}^2$ , the incident number of 9-keV photons at the detector is 2000 photons per pixel, or  $\sim 5$  photons/ $\mu\text{m}^2$ . The quantum efficiency of the micro-channel plate was assumed 1% in the further image modeling [10], shown in Section 4. The estimated peak signal level is about the same as used on ARIANE in implosions with DT neutron yields of  $Y_n \sim 10^{16}$  [7]. While ARIANE detects all x-rays in the range above  $\sim 7$  keV, M-ARIANE is designed to detect only a narrow band of x-rays around 9 keV. However, the x-ray emission is much brighter (about two-three orders of magnitude) at ignition yields of  $Y_n \sim 10^{18}$ , allowing to use a narrow-band x-ray detector without sacrificing quality of the imaging. While the x-ray signals significantly increase at ignition yields, the neutron-generated backgrounds also increase, requiring additional background mitigation, described in the next section.

## 3. NEUTRON-INDUCED BACKGROUNDS

The neutron-induced backgrounds have two main contributions [11,12]: direct energy deposition by charged particles (electrons, protons, alphas, heavy ion recoils, etc.) in the film; and the production of background light and signal attenuation through radiation-induced absorption in the optical image relay components [11-13]. In addition, there is cumulative damage of the glass components by long-term darkening [13-15]. Both optical and non-optical backgrounds are proportional to the dose of neutrons, charge particles and gammas at the detector location [11]. For example, the background level for the ARIANE detector has been predicted to be  $\sim 1.6$  optical density [7], corresponding to  $\sim 0.1$  erg/cm<sup>2</sup> of optical background on Kodak TMAX-3200 film for a shot with DT neutron yield of  $\sim 3 \times 10^{16}$  [7]. About half of this background is due to direct interactions of neutrons with film, while the other half is due to optical backgrounds generated in the P-11 phosphor and fiber-optic plate [6,7]. The framing camera in the ARIANE is located at 7 mm from the target chamber center, with direct, unshielded line of site to the target [7,8]. The framing camera in the M-ARIANE is shielded from neutrons and gamma rays by the target chamber wall and additional shielding, as shown in Fig. 1. One of the additional shields consists of 5-cm long, weighting 100 kg boron-polyethylene shield placed between the target chamber wall and the detector. In addition, the framing camera is placed within the 90-cm long shielding enclosure. The enclosure has 10-cm aperture to allow x-ray from the multilayer mirror to reach the framing camera. It consists of 10-cm thick, 500 kg lead shielding inside 20-cm thick, 300 kg boron-polyethylene shielding.

The calculated effect of the shielding is described in the Fig. 4 by comparing neutron and gamma exposures seen by the ARIANE detector (shown by the red color) and the M-ARIANE detector (shown by the blue color). Figure 4(a) shows the reduction of the neutron fluence as a function of the neutron energy, while the reduction of the gamma fluence is shown in Fig. 4(b). Both neutron and gamma fluences are significantly reduced by the shielding. Overall, the dose delivered to the detector is reduced by two orders of magnitude with the shielding. Thus, it is predicted that the background level for the M-ARIANE detector will be  $\sim 1.6$  optical density, corresponding to  $\sim 0.1$  erg/cm<sup>2</sup> of optical background on Kodak TMAX-3200 film for a shot with DT neutron yield of  $\sim 3 \times 10^{18}$ . The level of 0.1 erg/cm<sup>2</sup> is about 5 times below a maximum signal below the onset of saturation of the framing camera operated at phosphor voltage of 5 keV. This level of the background is acceptable for high-quality imaging as shown below in Section 4.

## 4. EFFECTS OF BACKGROUNDS ON IMAGE QUALITY

This Section presents modeling results of core images with the M-ARIANE. A simulated image of the implosion core with DT neutron yield of  $\sim 2 \times 10^{18}$  is shown in Fig. 2(a). It has been processed to include the effects of finite spatial resolution and statistical noise of the x-rays and MCP electrons.

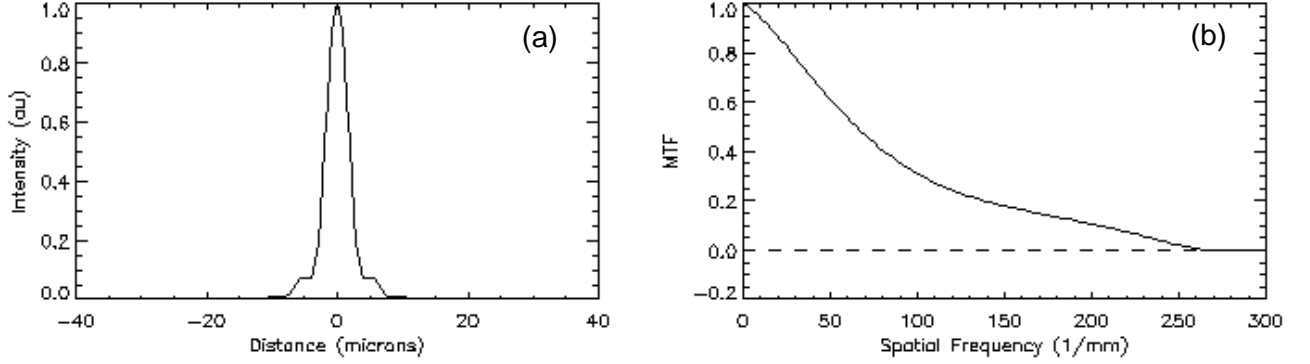


Figure 5: Calculated (a) lineout of the point-spread function (PSF) and (b) the modulation transfer function (MTF) of the M-ARIANE's 10- $\mu$ m diameter pinhole camera located at 27 cm from the target chamber center.

Figure 5(a) shows a lineout of the point-spread function (PSF) of the 10- $\mu$ m diameter pinhole, while the corresponding modulation transfer function (MTF) is shown in Fig. 5(b). Both pinhole PSF and MTF were calculated with the diffraction theory [16] using 9-keV x-rays and M-ARIANE's geometrical parameters; the distance between the object and the pinhole was 27 cm and the magnification of 36. Figure 6 shows measured MTF of the framing camera used in the image modeling [1].

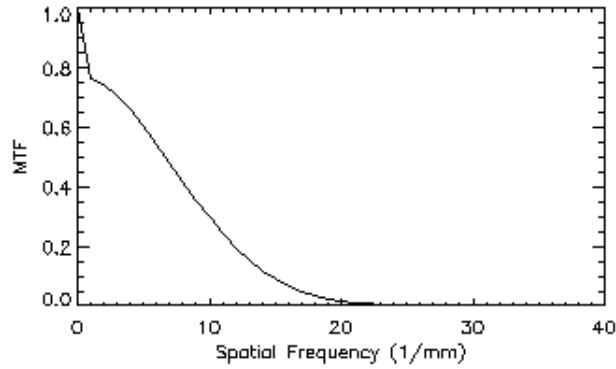


Figure 6: Measured modulation transfer function (MTF) of the M-ARIANE's framing camera.

Figure 7(a) shows a predicted framing-camera image including effects of spatial resolution and photon statistical noise of the x-rays and the framing camera, based on photo-metrics described in the earlier section. Figure 7(b) shows the image including additional effects of the neutron-generated noise in the framing camera. In this calculation, the peak signal was assumed  $0.5 \text{ erg/cm}^2$ , slightly below the onset of the saturation level of micro-channel plate at the phosphor voltage of 5 keV. The expected neutron-induced background level at the DT neutron yield of  $2 \times 10^{18}$  is below  $\sim 0.1 \text{ erg/cm}^2$ , as discussed in Section 2. In the image modeling, the peak signal is 5 times brighter than the average level of the neutron-induced background. The main features in the original image shown in Fig. 2(a) are still present in the final predicted image shown in Fig. 7(b), indicating that effects of the spatial resolution, photon noise, and neutron-induced backgrounds do not significantly distort main features of the original image. Figure 8 shows Fourier spectra of the signal and noise (solid curves) and noise (dashed curves), corresponding to the images without neutron-induced noise [shown in Fig. 8(a)] and with the neutron-induced noise [shown in Fig. 8(b)].

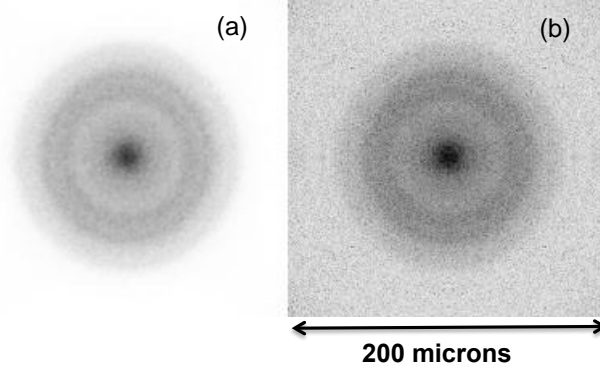


Figure 7: (a) Processed images including the effects of the spatial resolution and photon statistical noise, and (b) with additional neutron-induced background and noise in the shot with DT neutron yield of  $2 \times 10^{18}$ .

Comparing Figs. 8(a) and (b), noise is increased by  $\sim 3$  times when the neutron-induced backgrounds are included. The noise is affecting mostly signal at high spatial frequencies, around  $\sim 100 \text{ mm}^{-1}$ , which are close to a resolution limit of  $10 \text{ }\mu\text{m}$ .

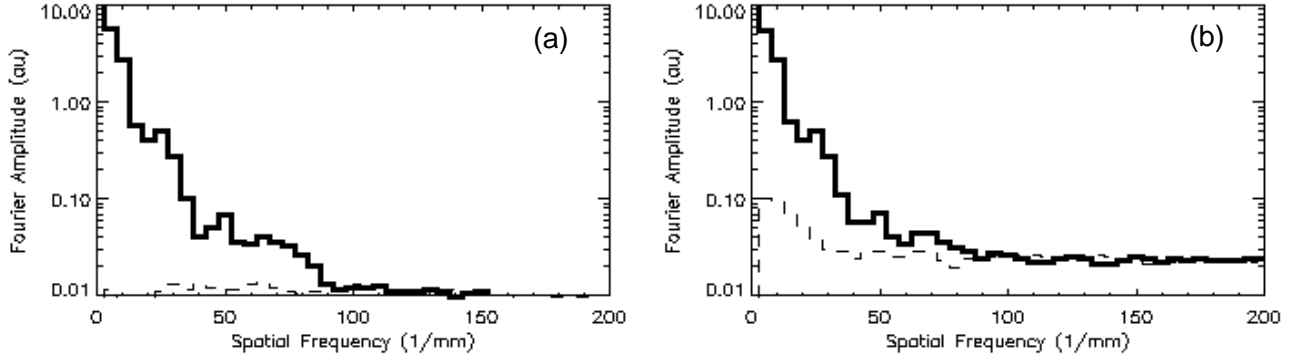


Figure 8: Fourier spectra of the signal with noise (thin solid curves), and the noise (dashed curves) as a function of the spatial frequency, corresponding to images (a) including effects of spatial resolution and photon statistical noise, and (b) with additional neutron-induced background and noise in a shot with DT neutron yield of  $2 \times 10^{18}$ .

## 5. SUMMARY

The effects of neutron-induced backgrounds were described in the gated imaging system M-ARIANE for the inertial confinement fusion (ICF). These backgrounds consist of mostly neutrons and gamma rays produced by inelastic scattering of neutrons. M-ARIANE, based on x-ray framing camera with film, has been designed to operate in such harsh neutron-induced background environments. Multilayer x-ray mirror and a shielding enclosure are the key components of this imaging system, designed to operate at ignition neutron yields of  $\sim 1 \times 10^{18}$  at National Ignition Facility (NIF).

## ACKNOWLEDGEMENTS

Lawrence Livermore National Laboratory is operated by Lawrence Livermore National Security, LLC, for the U.S. Department of Energy, National Nuclear Security Administration under Contract No. DE-AC52-07NA27344.

## REFERENCES

- [1] G.A. Kyrala, S. Dixit, S. Glenzer, D. Kalantar *et al.*, Rev. Sci. Instrum. **81**, 10E316 (2010).
- [2] G. H. Miller *et al.*, Nucl. Fusion **44**, S228 (2004).
- [3] E. I. Moses *et al.*, Phys. Plasmas **16**, 041006 (2009).
- [4] D.K. Bradley *et al.*, Rev. Sci. Instrum. **66**, 716 (1995).
- [5] C. J. Pawley and A. V. Deniz, Rev. Sci. Instrum. **71**, 1286 (2000).
- [6] N. Izumi, C. Hagmann, G. Stone *et al.*, Rev. Sci. Instrum. **81**, 10E515 (2010).
- [7] V. A. Smalyuk, J. Ayers, P. M. Bell *et al.*, SPIE Proceedings Vol. **8144**, Penetrating Radiation Systems and Applications XII, Gary P. Grim; Richard C. Schirato, Editors, p. 81440N (2011).
- [8] M. J. Ayers, B. Felker, V. A. Smalyuk *et al.*, in Target Diagnostics Physics and Engineering for Inertial Confinement Fusion, Perry Bell, Gary P. Grim, Editors, Proceedings of SPIE Vol. **8505** (SPIE, Bellingham, WA 2012), 85050J (2012).
- [9] P.M. Bell, D.K. Bradley, J.D. Kilkenny *et al.*, Rev. Sci. Instrum. **81**, 10E540 (2010).
- [10] B. L. Henke, J. P. Knauer, and K. Premaratne, J. Appl. Phys. **52**, 1509 (1981).
- [11] N. Izumi, J. Emig, J. Moody *et al.*, SPIE Proceedings Vol. **8142**, Hard X-Ray, Gamma-Ray, and Neutron Detector Physics XIII, Larry A. Franks; Ralph B. James; Arnold Burger, Editors, 81420I (2011).
- [12] C. Hagmann, J. Ayers, P. M. Bell *et al.*, SPIE Proceedings Vol. **8144**, Penetrating Radiation Systems and Applications XII, Gary P. Grim; Richard C. Schirato, Editors, p. 814408 (2011).
- [13] Schott North America, 122 Charlton St., Southbridge, MA 01550.
- [14] C. Hagmann, N. Izumi, P. Bell *et al.*, Rev. Sci. Instrum. **81**, 10E514 (2010).
- [15] E.J. Friebele, G.H. Sigel, Jr. and M.E. Gingerich, IEEE TNS 25, 1261 (1978).
- [16] V. A. Smalyuk *et al.*, Rev. Sci. Instrum. **72**, 635–642 (2001).